RM E56I26

NACA RM E56I26

NACA

RESEARCH MEMORANDUM

PERFORMANCE OF A SUPERSONIC RAMP-TYPE SIDE INLET WITH RAM-SCOOP THROAT BLEED AND VARYING FUSELAGE BOUNDARY-LAYER REMOVAL MACH NUMBER RANGE 1.5 TO 2.0

By Glenn A. Mitchell and Robert C. Campbell

Lewis Flight Propulsion Laboratory
Cleveland, Ohio

NATIONAL ADVISORY COMMITTEE
FOR AERONAUTICS

WASHINGTON

January 17, 1957

NATIONAL ADVISORY COMMITTEE FOR AERONAUTICS

RESEARCH MEMORANDUM

PERFORMANCE OF A SUPERSONIC RAMP-TYPE SIDE INLET WITH RAM-SCOOP THROAT BLEED AND VARYING FUSELAGE BOUNDARY-LAYER REMOVAL MACH NUMBER RANGE 1.5 TO 2.0

By Glenn A. Mitchell and Robert C. Campbell

SUMMARY

An experimental investigation of combinations of ram-scoop throat bleed and fuselage boundary-layer removal for a fuselage-mounted 14° ramp inlet was conducted at Mach numbers of 1.5, 1.8, and 2.0.

Provided sufficient throat bleed was employed, maximum pressure recoveries of 0.87 to 0.88 at a Mach number of 2.0 were obtained regardless of the amount of fuselage boundary layer ingested by the inlet. Side fairings on the inlet further increased the maximum recovery to 0.90 and 0.91 while decreasing critical drag coefficients as much as 8 percent and increasing critical mass-flow ratios as much as 5 percent. Peak pressure recoveries were comparable for two axial positions of the scoop-type bleed. Calculations indicate that with optimum throat bleed, thrust-minus-drag was highest without fuselage boundary-layer removal ahead of the inlet.

INTRODUCTION

Ramp boundary-layer separation has been observed on a number of side inlets, and steps have been taken to bleed off this boundary layer in the region of the inlet throat. Improvements in net-thrust-minus-drag have been shown in cases where inlet throat boundary-layer removal was employed (refs. 1 to 4), even when the fuselage boundary layer ahead of the inlet was removed. Three basic bleed types have been investigated: (1) a perforated surface, (2) a flush slot, and (3) a ram scoop.

Reference 4 indicates that with flush slot bleed at the throat, it was possible to maintain or increase over-all thrust-minus-drag performance while decreasing the amount of fuselage boundary layer removed ahead of the inlet. As an extension of the work of reference 4, a study was made to evaluate the effectiveness of a ram-scoop bleed at the throat of

the 14° ramp inlet of that reference. Combinations of fuselage and inlet throat boundary-layer removal similar to those of reference 4 were investigated with and without inlet side fairings for two axial positions of the ram scoop. Included in this investigation are data for an 18° ramp inlet which was believed to reduce or eliminate the separation behind the inlet terminal shock. The model was tested at zero angle of attack and free-stream Mach numbers of 1.5, 1.8, and 2.0.

SYMBOLS

A	area, sq in.
$A_{B,min}$	internal-bleed minimum-flow area, sq in.
A_F	maximum frontal area of basic configuration, 0.759 sq ft
A_i	inlet capture area, 19.51 sq in.
A_{th}	inlet throat area, 13.55 sq in. for 14° ramp inlet, 12.76 sq in. for 18° ramp inlet
A_2	diffuser area at model station 85.0, 22.96 sq in.
C_D	drag coefficient, $\frac{D}{q_0 A_F}$
D	configuration drag, lb
ΔD	incremental drag, $D - D_b$, lb
F	internal thrust of turbojet-engine and inlet combination, lb
h	fuselage boundary-layer diverter height, in.
$\frac{m_3}{m_0}$	main-duct mass-flow ratio, $\frac{\text{main-duct mass flow}}{\rho_0 V_0 A_i}$
P	total pressure
$P_{2,max} - P_{2,min}$	maximum total-pressure variation across pressure rake at station 85.0
$\frac{P_{2,max} - P_{2,min}}{P_2}$	total-pressure distortion

q_0	free-stream dynamic pressure, $\frac{1}{2}\rho_0 V_0^2$
t	fuselage boundary-layer thickness, approx. 0.55 in.
V	velocity, ft/sec
$\left(\frac{w\sqrt{\theta}}{\delta A}\right)_2$	weight flow per unit area, referenced to standard sea-level conditions, (lb/sec)/sq ft
δ	ratio of total pressure to NACA standard sea-level total pressure of 2116.22 lb/sq ft
θ	ratio of total temperature to NACA standard sea-level temperature of 518.688° R
ρ	mass density

Subscripts:

b	basic configuration: 14° ramp inlet, smooth-contour diffuser (ram scoop closed) with side fairings, at h/t = 1
max	maximum
min	minimum
0	free stream
2	diffuser total-pressure survey station, model station 85.0
3	diffuser static-pressure survey station, model station 99.2

APPARATUS AND PROCEDURE

A schematic drawing of the fuselage, inlet, and boundary-layer-removal system for the 14° ramp with the aft ram scoop is illustrated in figure 1, and photographs of the model appear in figure 2. An 18° ramp inlet with an internal cowl lip angle of 18° replaced the 14° ramp inlet during part of this investigation. The inlet-diffuser assembly was mounted on the flat underside of a basic body-of-revolution consisting of an ogive nose and a 10-inch-diameter cylindrical afterbody downstream of model station 46.2. For all configurations the inlet cowl lip was located

at model station 61.9. Swept side fairings, when used on the inlet, extended from the cowl sides to the leading edge of the ramp.

The fuselage boundary-layer diverter height was varied with spacers inserted between the body and the inlet-diffuser installation. The diffuser reference line was maintained parallel to the body axis at all times.

The bleed scoops of this investigation and the flush slot of reference 4 were located on the ramp side of the inlet and extended from wall to wall. The minimum-flow area of the bleed passage was located at the bleed inlets of the ram-scoop configurations and at the bleed exit of the flush slot configuration of reference 4.

The ram scoop was formed by a section of the diffuser floor hinged at its downstream end. Variations in scoop-inlet area (and, consequently, bleed mass flow) were accomplished by rotating this section of the floor, in trap-door fashion, about its hinge line. The scoop leading-edge radius was 0.01 inch for the ram scoops, compared to a leading-edge radius of 0.04 inch for the flush bleed. Mass flow drawn into the bleed passage was ejected through openings in either side of the inlet cowl.

Zero bleed mass flow through the flush slot of reference 4 was accomplished by closing the bleed exit, while the bleed passage remained vented to the diffuser at the bleed inlet slot. However, the completely closed ram scoop presented a typical smooth-contour diffuser to the passing flow. The aft ram-scoop leading edge was located 4.03 inches (more than 1 hydraulic diam.) downstream of the cowl lip. The forward ram-scoop leading edges were located 0.65 and 0.78 inch from the cowl lip for the 14° and 18° ramps, respectively.

The diffuser area variations for the 14° and 18° ramps are shown in figure 3. Area variations resulting from typical open positions of the forward and aft ram scoops are represented by the dashed lines.

The model was connected to the support sting by a strain-gage balance that measured axial forces. Inlet mass flow was varied by means of a remotely controlled movable tailpipe plug attached to the sting.

Pressure instrumentation consisted of a flow-field survey rake ahead of the inlet at model station 55.1, total-pressure tubes and static-pressure orifices at station 85.0 in the diffuser, static-pressure orifices at station 99.2 in the diffuser, base-pressure orifices, and chamber-pressure orifices located in the model-balance cavity. The outermost total-pressure tubes at station 85.0 were located 0.2 inch from the wall, or at 0.927 of the duct radius.

The main-duct mass-flow ratio was determined from the static-pressure measurements at station 99.2 and the known area ratio between that station and the exit plug where the flow was assumed to be choked. Average total pressure was calculated by area-weighting the total-pressure measurements. The forces resulting from the change in inlet-air momentum from free stream to diffuser exit, and base forces resulting from the difference in base pressures from the free-stream static pressure have been excluded from the model force data.

The model was tested at zero angle of attack and free-stream Mach numbers of 1.5, 1.8, and 2.0 with a maximum of four external diverter heights for each configuration. The configurations investigated and the fuselage diverter heights at which each was tested are listed in the following table:

Configuration designation	Ramp angle, deg	Side fairings	Bleed configuration	Fuselage diverter height (fraction of boundary-layer thickness), h/t	Figure number
A-1	14	Off	Forward ram scoop	1, $\frac{2}{3}$, $\frac{1}{3}$, 0	4
B-1	14	Off	Aft ram scoop	1	5
C-1	18	Off	Forward ram scoop	1, $\frac{1}{3}$	8
A-2	14	On	Forward ram scoop	1, $\frac{1}{3}$, 0	6
B-2	14	On	Aft ram scoop	1, $\frac{2}{3}$, $\frac{1}{3}$	7
C-2	18	On	Forward ram scoop	1, $\frac{1}{3}$	9

At each diverter height and Mach number, the main-duct mass-flow ratio was varied for several inlet throat-bleed minimum-flow areas. The Reynolds number was approximately 4.5×10^6 per foot. The Mach number ahead of the inlet, as determined from the survey rake at station 55.1, was within +0.02 of the free-stream Mach number, and the fuselage boundary-layer thickness, also determined from this rake, was 0.55 inch at the Mach numbers tested.

RESULTS AND DISCUSSION

Inlet performance characteristics, consisting of diffuser total-pressure distortion, total-pressure recovery, and external drag coefficient, are presented in figures 4 to 9. These data are plotted as a function of main-duct mass-flow ratio for several combinations of fuselage and inlet throat boundary-layer removal. In several cases where data are lacking, the dashed lines indicate extrapolations used in the subsequent calculations of thrust-minus-drag.

Improvements in both pressure recovery and distortion by inlet throat bleeding were observed at all Mach numbers and fuselage diverter heights for all configurations tested. In general, both critical and peak pressure recoveries were increased by inlet throat bleed, though the increase in critical pressure recovery was frequently not as great as the increase in peak pressure recovery. In all instances except one, peak pressure recoveries obtained with inlet throat bleed at reduced fuselage diverter heights were as good as or better than the peak recoveries obtained at the maximum diverter height. The exception, configuration C-2 at a Mach number of 1.8 (fig. 9(b)), probably occurred because sufficient bleed area was not tested in that instance.

The pressure distortions obtained with inlet throat bleed were generally comparable at all fuselage diverter heights for any given configuration and Mach number.

Some effects of ram-scoop bleed location on the pressure recovery of the 14° ramp inlet without side fairings are found in figures 4 and 5. The peak pressure recoveries with throat bleed were generally comparable, although obtained at slightly different mass-flow ratios for the two configurations (A-1 and B-1), and at a Mach number of 2.0 were about 0.87 to 0.88. With the addition of inlet side fairings (figs. 6 and 7) peak pressure recoveries of the two configurations were still within 0.01 to 0.02 where sufficient bleed flow areas were tested, and at a Mach number of 2.0 were increased to 0.90 and 0.91.

At comparable mass-flow ratios, little effect of the addition of side fairings could be found on the level of pressure distortions. It appears, however, that for the 14° ramp inlet configurations (figs. 4 to 7) the appropriate use of inlet throat bleed reduced inlet critical pressure distortions to between 5 and 10 percent of the average diffuser total pressure as compared to 15 percent and greater without throat bleed. Similar reductions in inlet critical pressure distortions were observed for the flush bleed of reference 4. Distortions of the 18° ramp inlet were higher than those of the 14° ramp inlet.

The boundary layer on the 14° ramps of this investigation was observed to separate behind the inlet terminal shock. An 18° ramp inlet

having a reduced ramp Mach number was then investigated. Though the pressure rise across the inlet terminal shock generally tends to thicken the ramp boundary layer, this 18° ramp did not exhibit the extensive separation noted on the 14° ramp. A comparison of the relative effect of ramscoop bleed on the performance of the two compression angles (configurations A-1, A-2, C-1, and C-2) is illustrated in figures 4, 6, 8, and 9. Without inlet throat bleed, both ramps generally had about the same pressure recovery for the Mach numbers and fuselage diverter heights tested. While the 14° ramp inlet had separation, it also had the advantage of a second oblique shock, and apparently these effects tended to counterbalance each other. Throat bleed generally improved the peak pressure recoveries of the 14° ramp inlet slightly more than it did for the 18° ramp inlet.

The critical main-duct mass-flow ratios without internal bleed decrease with decreasing fuselage diverter height (figs. 4 to 9). The reduction in critical mass-flow ratio from its value at the maximum external diverter height is, in most cases, very close to the theoretical mass-flow decrement predicted for a fuselage boundary layer with a 1/7-power velocity ratio profile (ref. 5). However, critical mass flows for the 14° ramp with side fairings and no fuselage boundary-layer removal were reduced more than the theoretically predicted mass-flow decrement because of spillage behind the ramp leading-edge oblique shock at Mach numbers of 1.8 to 2.0. The addition of side fairings to the 14° ramp inlet at Mach numbers of 1.8 and 2.0 increased the critical mass-flow ratio without internal bleed about 3 to 5 percent, down to diverter heights of one-third the boundary-layer thickness. In other cases, the addition of side fairings generally had little effect on critical mass-flow ratios without throat bleed.

The data of figures 4 to 9 generally were obtained by reducing the main-duct mass-flow ratio until the inlet terminal shock and the diffuser static pressure (station 85.0) were observed to oscillate. The extension of some curves to the left of the last symbol indicates that such oscillations were not observed in that case. Occasionally, quantitative data were taken of the amplitudes of the pressure fluctuations. The numerals adjacent to the tailed symbols on the pressure-recovery - mass-flow plots of figures 4 to 9 indicate the total amplitude of the fluctuations to the nearest percent of diffuser total pressure. Where no numerals appear, data on these amplitudes were not available.

From the curves of drag coefficient shown in these figures, it is evident that the minimum drag decreased for decreasing fuselage diverter height. These curves also show that the minimum drag for configurations with side fairings was lower than that for similar configurations without side fairings. For example, the minimum drag coefficient for the 14° ramp inlet decreased 3 to 8 percent with the addition of side fairings. However, a large percentage of this decrease in the minimum drag coefficient

was due to the increase in capture mass flow obtained with the addition of side fairings. Without the side fairings, the drag rise obtained by bleeding at the inlet throat (differences between minimum drag coefficients at successive bleed-minimum-flow-area ratios $A_{B,min}/A_{th}$) was somewhat less than the subcritical drag rise for the same amount of mass-flow spillage. With the side fairings installed, the increase in drag for internal bleeding was slightly greater than the subcritical drag rise for the smaller amounts of bleed. However, with larger amounts of bleed ($A_{B,min}/A_{th}$ = 0.16 or greater), the drag rise was equal to or less than the subcritical drag rise. In comparing these bypass drags with those of the flush slot of reference 4, it was noted that the bypass drags of the ram-scoop configurations were generally higher than those of the flush slot configuration.

Inlet-engine thrust-minus-drag was computed to determine the overall performance of each configuration for the combinations of boundary-layer removal investigated. Thrusts were obtained for a typical turbojet engine assumed to be operating at 35,000 feet with maximum afterburning. At each Mach number and fuselage diverter height, the inlet and engine were matched over the mass-flow range of each configuration. The maximum thrust-minus-incremental-drag values obtained are presented in figure 10 as a percent of the maximum thrust of the basic configuration. Incremental drag represents the difference between the drag of a given configuration and that of the basic configuration. The basic configuration is defined as the 14° ramp inlet with the smooth-contour diffuser (ram scoop closed) and side fairings (figs. 6(a) and 7(a)) at an external diverter height equal to the fuselage boundary-layer thickness (h/t = 1). The thrust-minus-drag values for the flush slot of reference 4 are included in figure 10 to facilitate comparisons. The thrusts of the basic configuration of this report and those of reference 4 are identical at Mach numbers of 2.0 and 1.8, but differ slightly at a Mach number of 1.5. The thrust-minus-drag values of reference 4 are corrected for this difference in figure 10. In all cases, external drag coefficients and model frontal areas were assumed to remain constant for the changes in inlet size required to accommodate changes in diffuser weight flow.

The optimum amount of inlet throat bleed at each fuselage diverter height is defined herein as that which affords the maximum thrust-minus-drag. These maximum net-thrust ratios are presented in figure 10 as a function of the fuselage diverter height parameter. For the 14° ramp configurations investigated, optimum internal bleed provided net thrusts over the full range of fuselage diverter height that were equal to or greater than the thrusts of the basic configuration. For most configurations (both 14° and 18° ramps) the optimum combination of fuselage and inlet throat boundary-layer removal provided the highest thrusts at the lowest fuselage diverter height. The flush slot of reference 4 in general showed

net thrusts higher than those of the ram scoops reported herein. Net thrusts for the two positions of the ram scoops were within 1 to 2 percent of each other. At Mach numbers of 2.0 and 1.8 the net thrusts of configuration A without side fairings were 1 to 5 percent less than those obtained with side fairings. The maximum thrust ratios obtained with the 18° ramp configurations were at best about equal to the lowest obtained with the 14° ramp configurations, and in some cases were as much as 5 percent lower. Maximum thrust gains obtained with bleed over the Mach number range were about 8 percent of the thrust of the basic configuration without internal bleed at the maximum fuselage diverter height.

SUMMARY OF RESULTS

An experimental investigation to evaluate ram-scoop throat bleed in combination with several degrees of fuselage boundary-layer removal was conducted in the Lewis 8- by 6-foot supersonic wind tunnel at Mach numbers of 1.5, 1.8, and 2.0. The following results were obtained:

1. Provided sufficient throat bleed was employed, the maximum pressure recovery of a 14° ramp inlet was 0.87 to 0.88 at a Mach number of 2.0 regardless of the amount of fuselage boundary-layer removal.

2. Inlet side fairings increased the maximum recovery with throat bleed to 0.90 and 0.91 at a Mach number of 2.0 regardless of the amount of fuselage boundary-layer removal. Side fairings decreased the critical drag coefficient as much as 8 percent and increased the critical mass-flow ratio as much as 5 percent.

3. With throat bleed, peak pressure recoveries and calculated thrust-minus-drag values were within 1 to 2 percent for two longitudinal positions of the ram scoop.

4. Calculations indicate that with optimum throat bleed, thrust-minus-drag was highest without fuselage boundary-layer removal ahead of the inlet.

Lewis Flight Propulsion Laboratory
National Advisory Committee for Aeronautics
Cleveland, Ohio, October 10, 1956

REFERENCES

1. Campbell, Robert C.: Performance of a Supersonic Ramp Inlet with Internal Boundary-Layer Scoop. NACA RM E54I01, 1954.

2. Obery, Leonard J., and Cubbison, Robert W.: Effectiveness of Boundary-Layer Removal Near Throat of Ramp-Type Side Inlet at Free-Stream Mach Number of 2.0. NACA RM E54I14, 1954.

3. Allen, John L., and Piercy, Thomas G.: Performance Characteristics of an Underslung Vertical-Wedge Inlet with Porous Suction at Mach Numbers of 0.63 and 1.5 to 2.0 NACA RM E56B15, 1956.

4. Campbell, Robert C.: Performance of Supersonic Ramp-Type Inlet with Combinations of Fuselage and Inlet Throat Boundary-Layer Removal. NACA RM E56A17, 1956.

5. Simon, Paul C., and Kowalski, Kenneth L.: Charts of Boundary-Layer Mass Flow and Momentum for Inlet Performance Analysis - Mach Number Range, 0.2 to 5.0. NACA TN 3583, 1955.

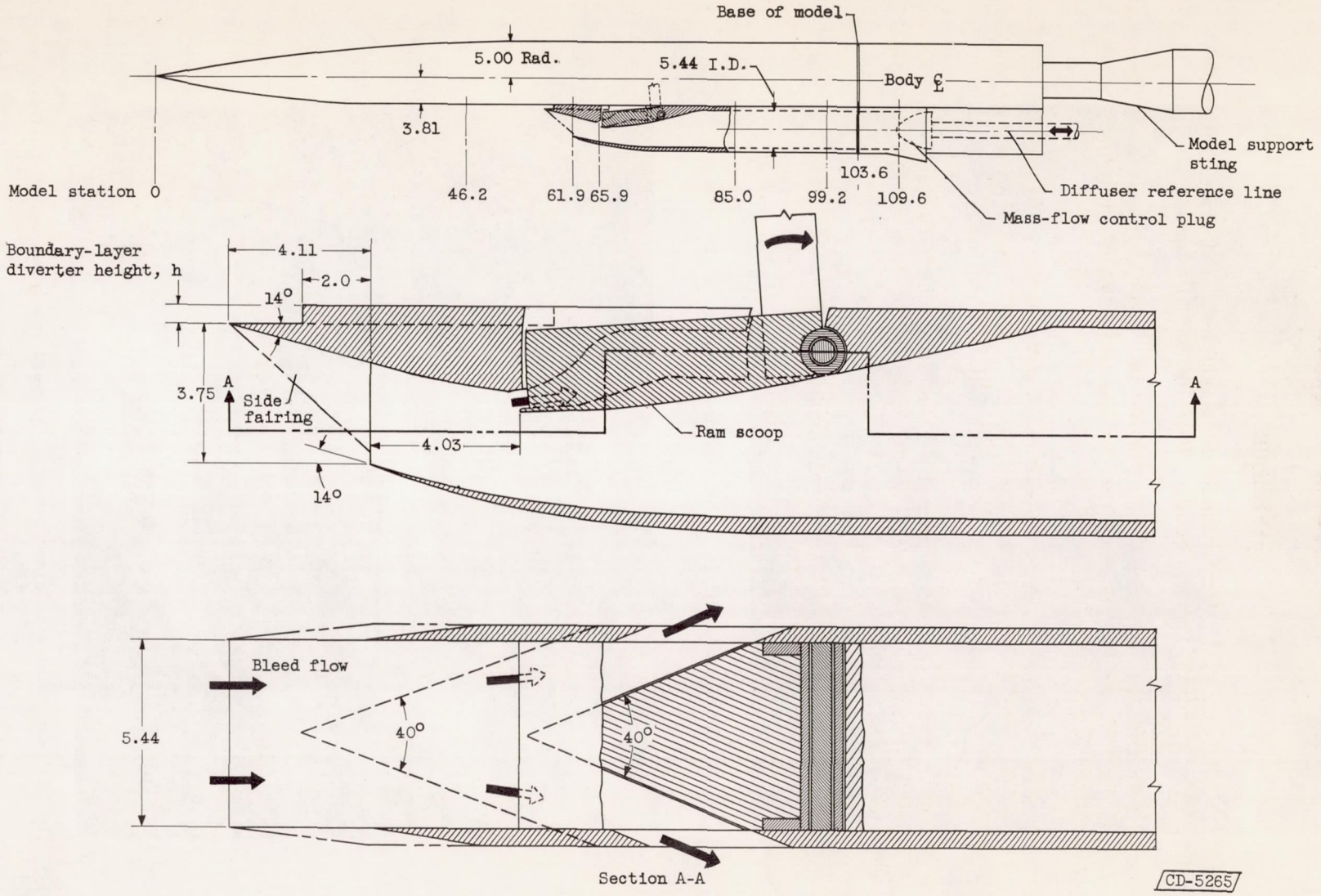

Figure 1. - Schematic drawing of model and inlet with 14° ramp and aft ram scoop. (All dimensions in inches except where noted.)

CONFIDENTIAL

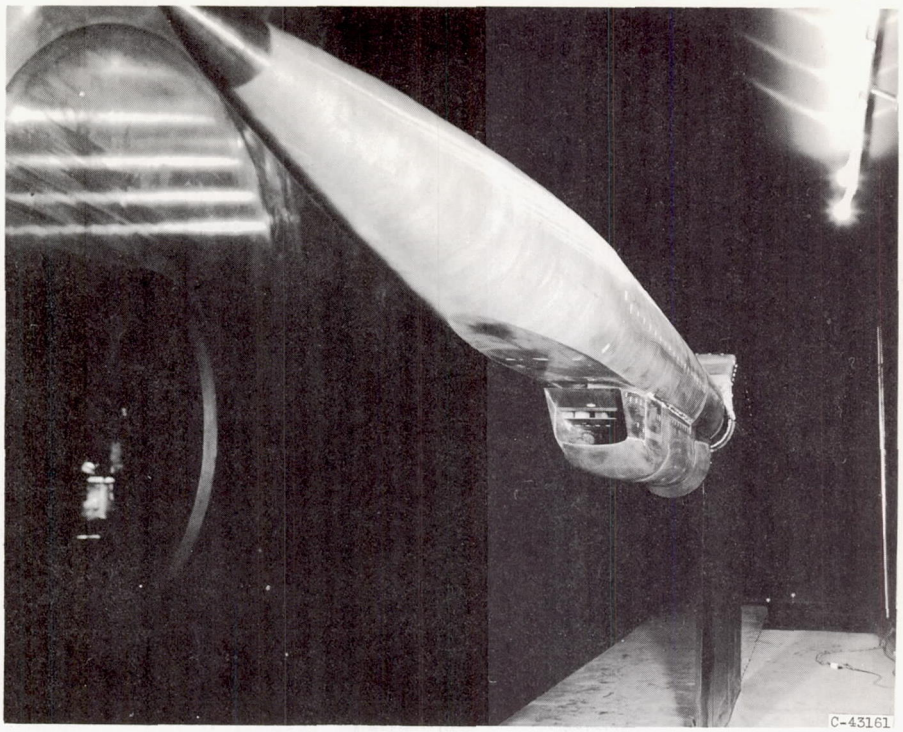

(a) Model installed in 8- by 6-foot supersonic wind tunnel.

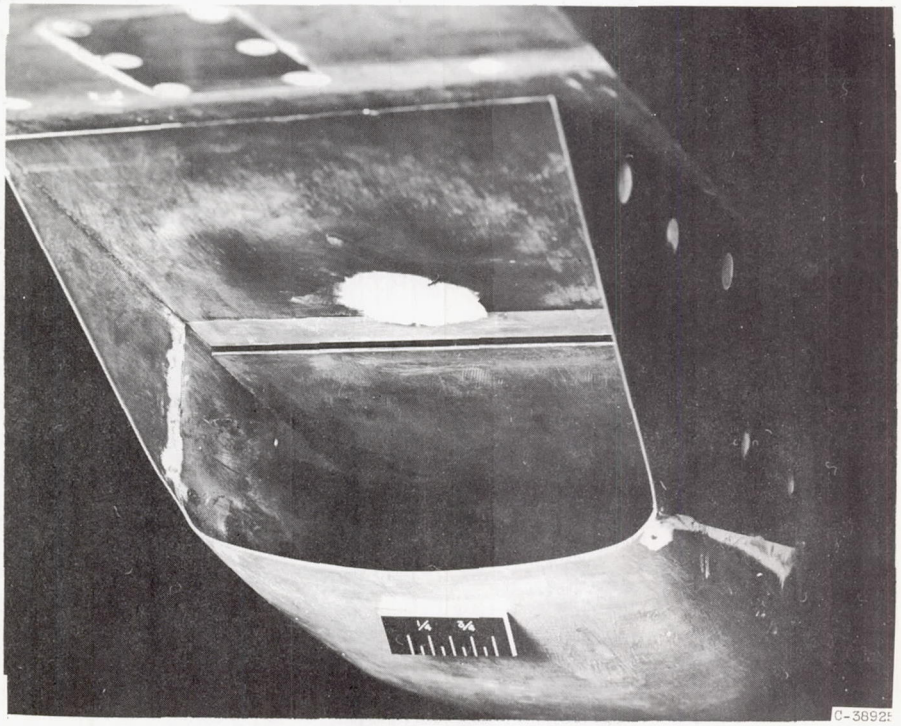

(b) 14° Ramp inlet with side fairings. Forward ram scoop nearly closed.

Figure 2. - Photographs of model.

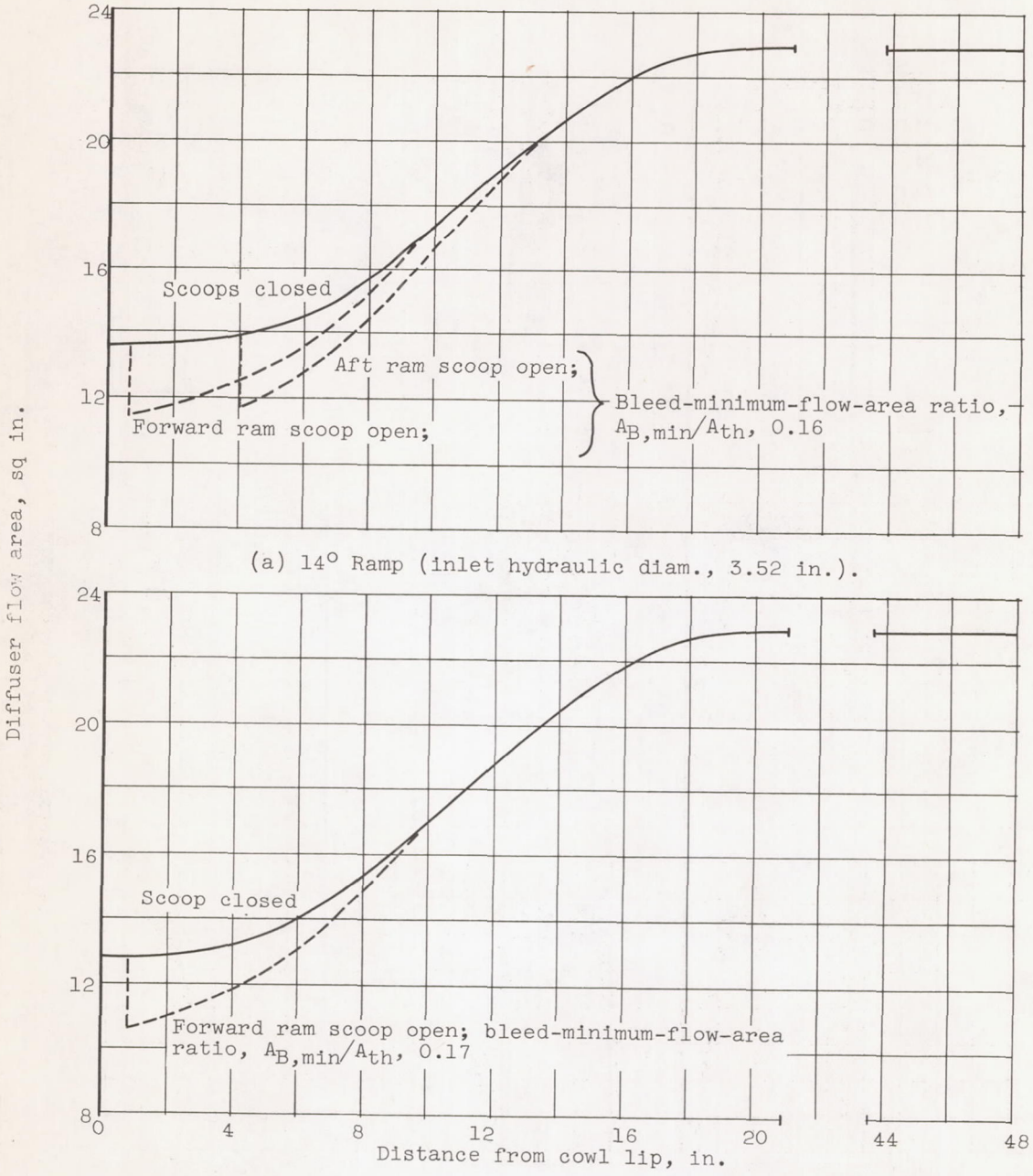

(a) 14° Ramp (inlet hydraulic diam., 3.52 in.).

(b) 18° Ramp (inlet hydraulic diam., 3.35 in.).

Figure 3. - Subsonic diffuser area variation.

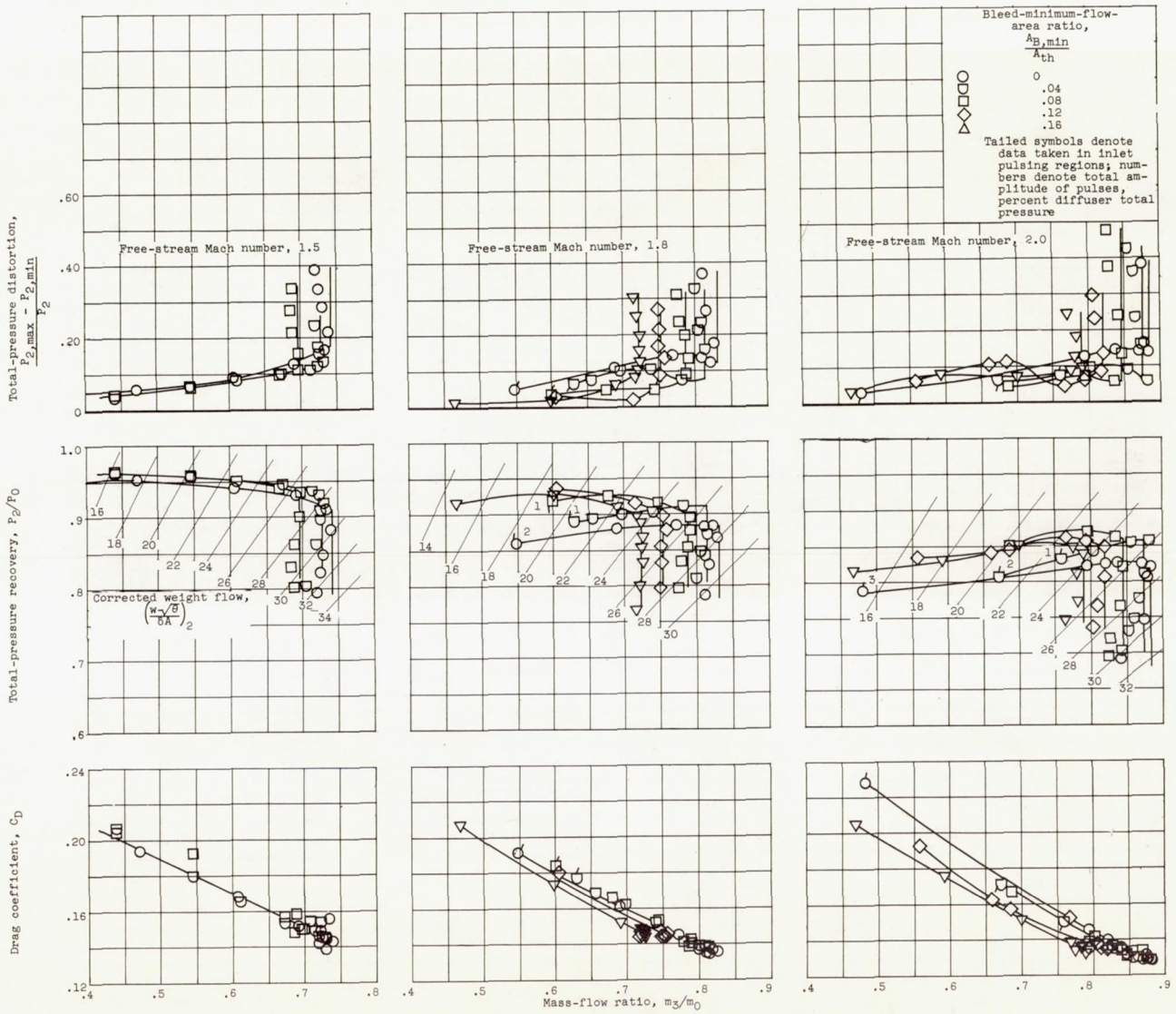

(a) External diverter height parameter, h/t, 1.

Figure 4. - Inlet performance characteristics of forward ram scoop having 14° ramp without side fairings (configuration A-1).

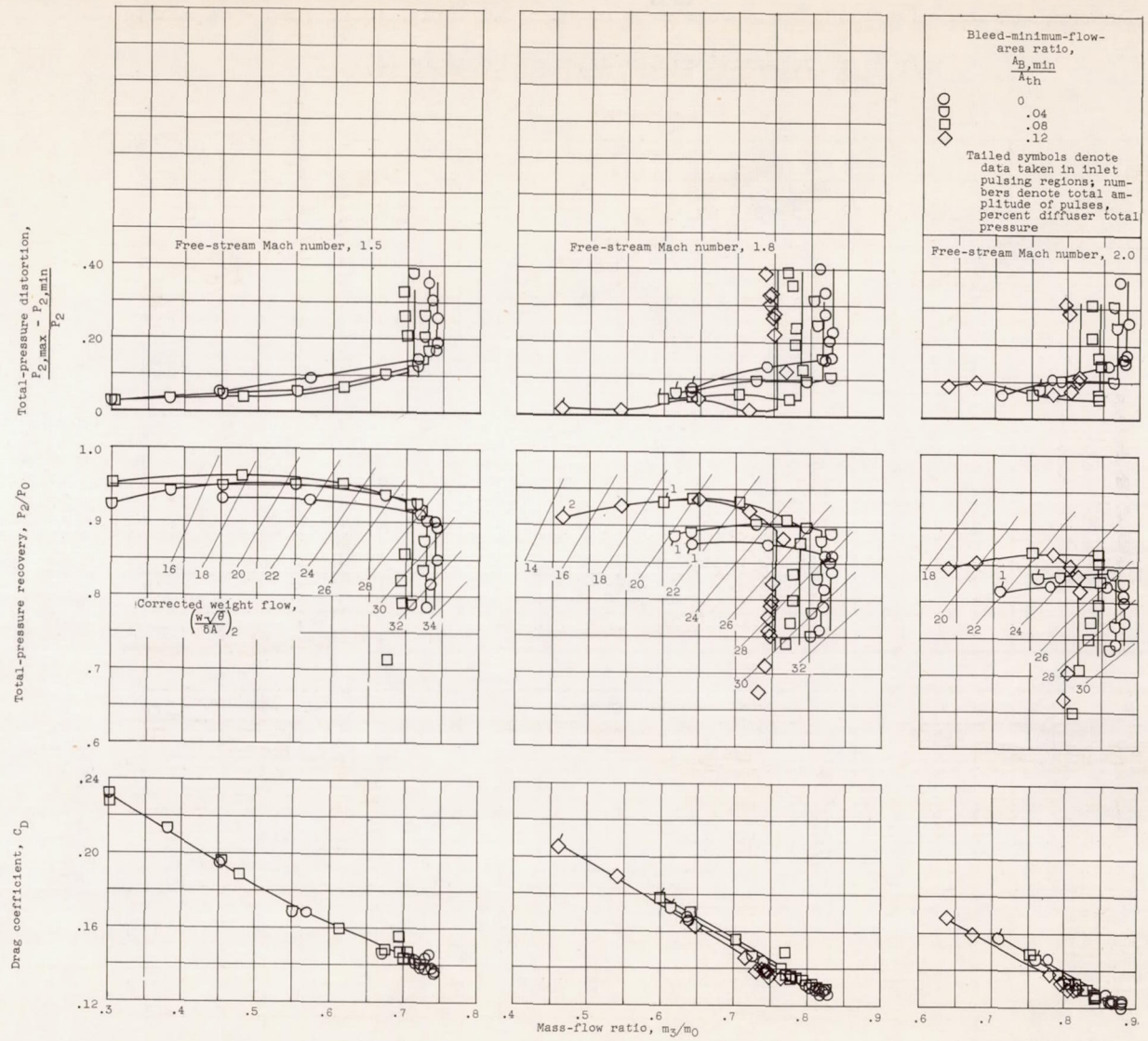

(b) External diverter height parameter, h/t, 2/3.

Figure 4. - Continued. Inlet performance characteristics of forward ram scoop having 14° ramp without side fairings (configuration A-1).

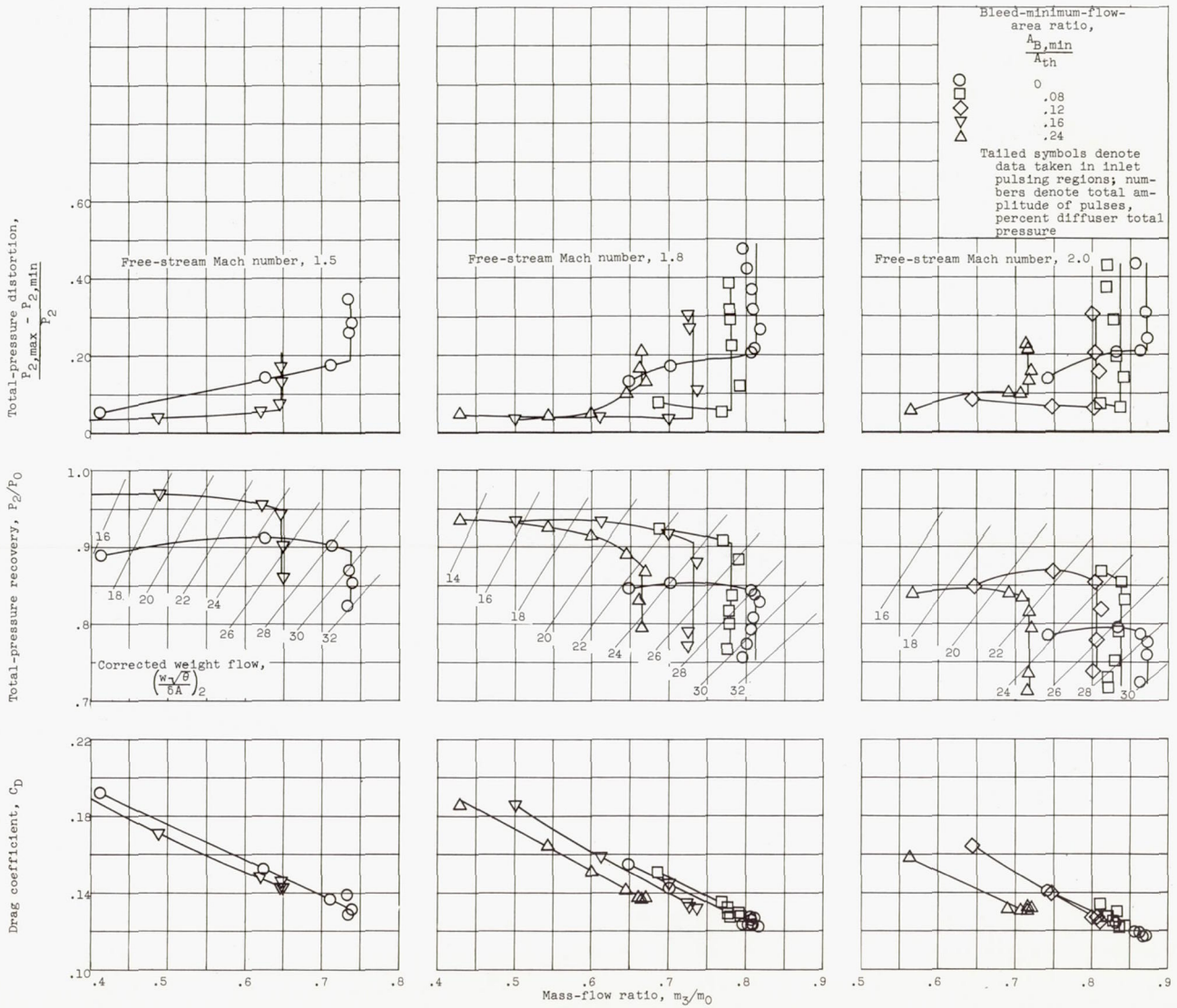

(c) External diverter height parameter, h/t, 1/3.

Figure 4. - Continued. Inlet performance characteristics of forward ram scoop having 14° ramp without side fairings (configuration A-1).

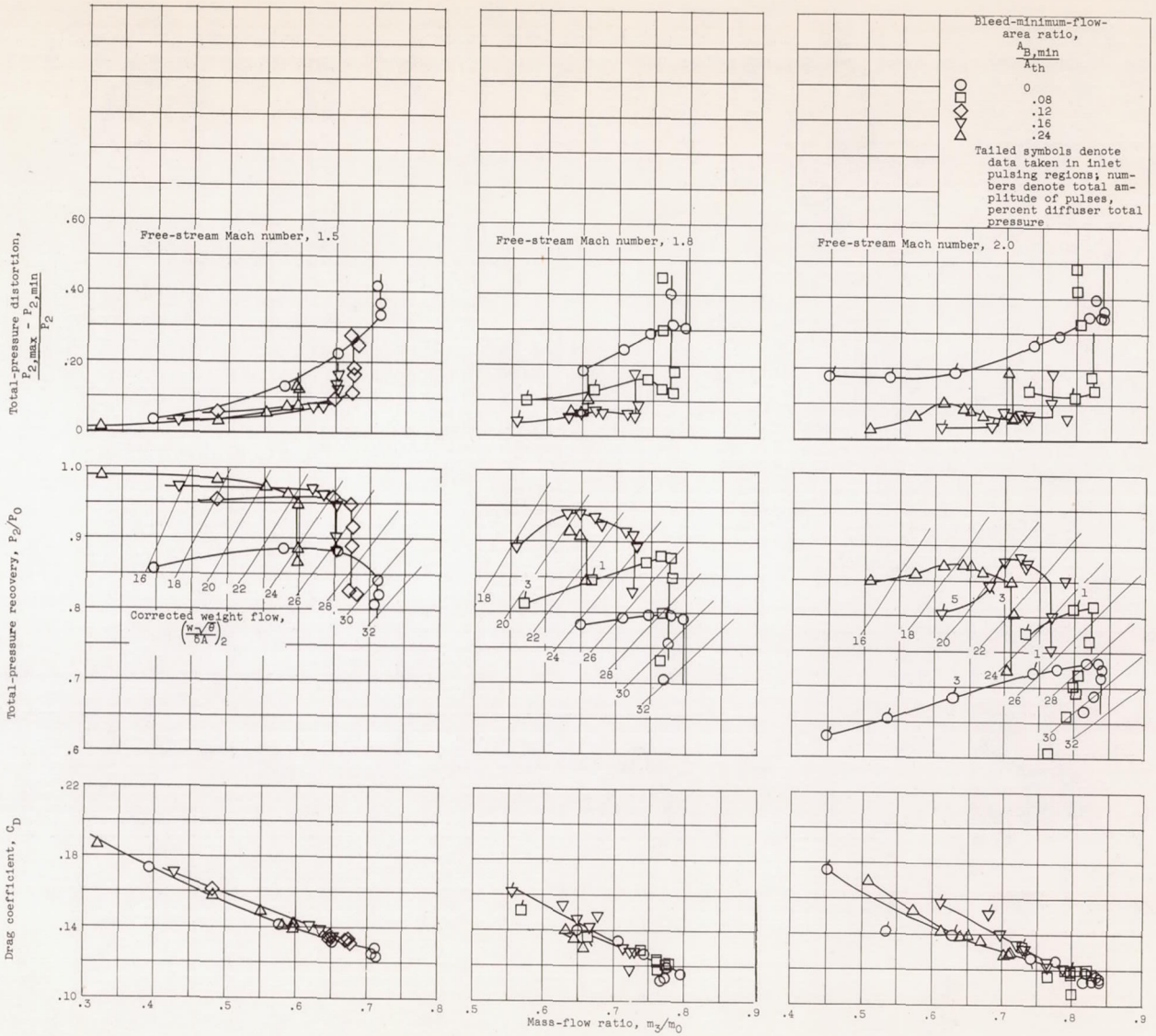

(d) External diverter height parameter, h/t, 0.

Figure 4. - Concluded. Inlet performance characteristics of forward ram scoop having 14° ramp without side fairings (configuration A-1).

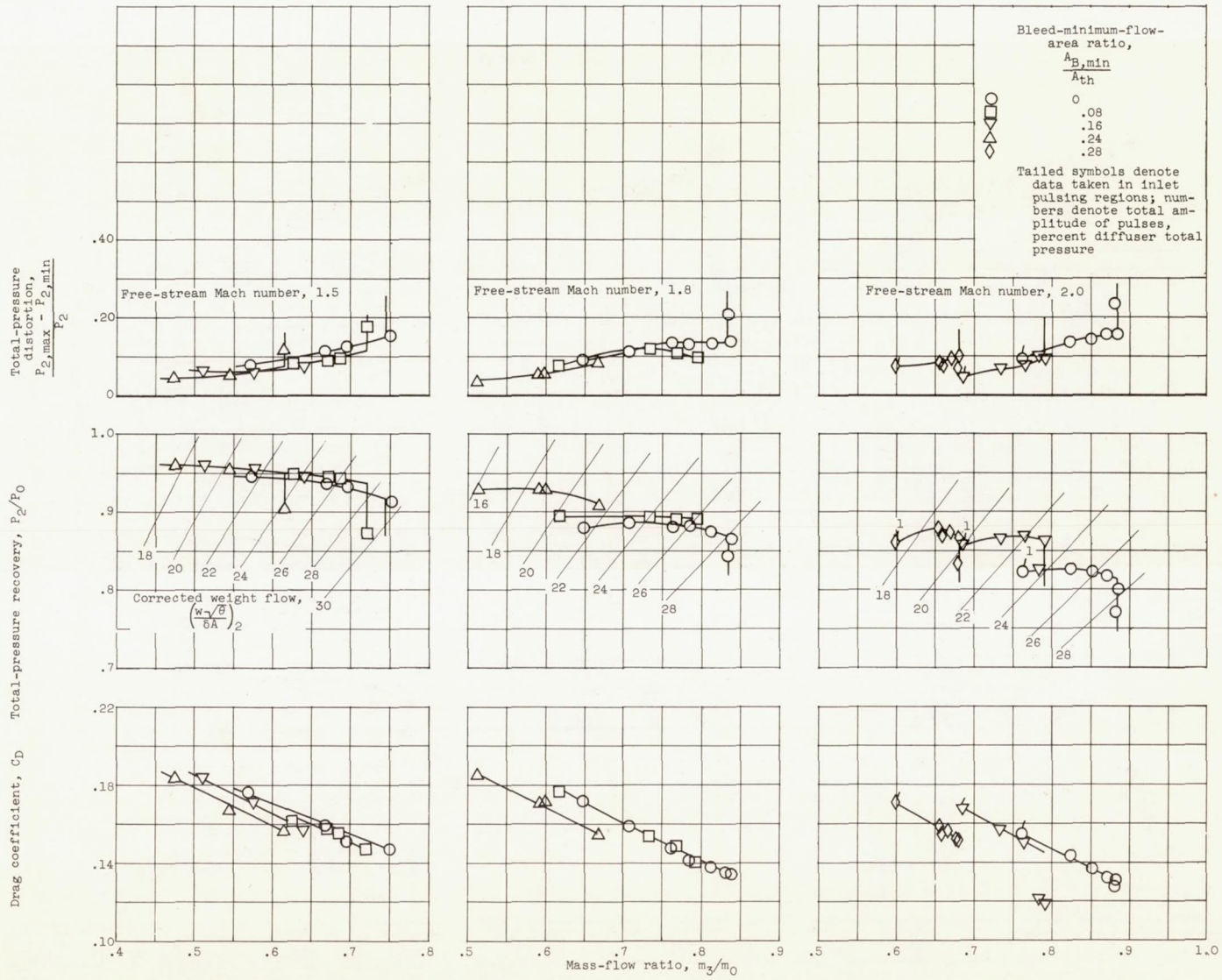

Figure 5. - Inlet performance characteristics of aft ram scoop having 14° ramp without side fairings (configuration B-1). External diverter height parameter, h/t, 1.

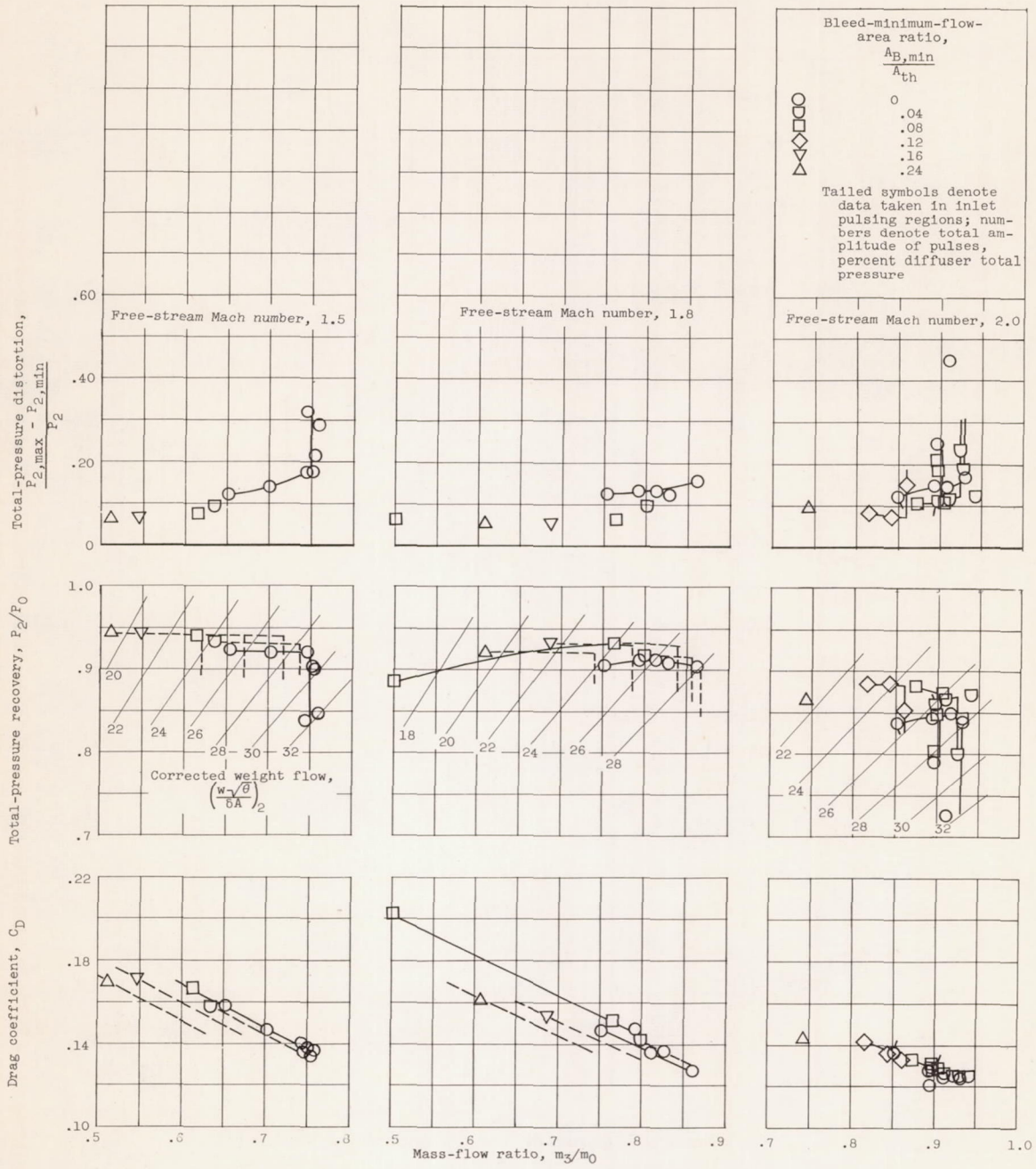

(a) External diverter height parameter, h/t, 1.

Figure 6. - Inlet performance characteristics of forward ram scoop having 14° ramp with side fairings (configuration A-2).

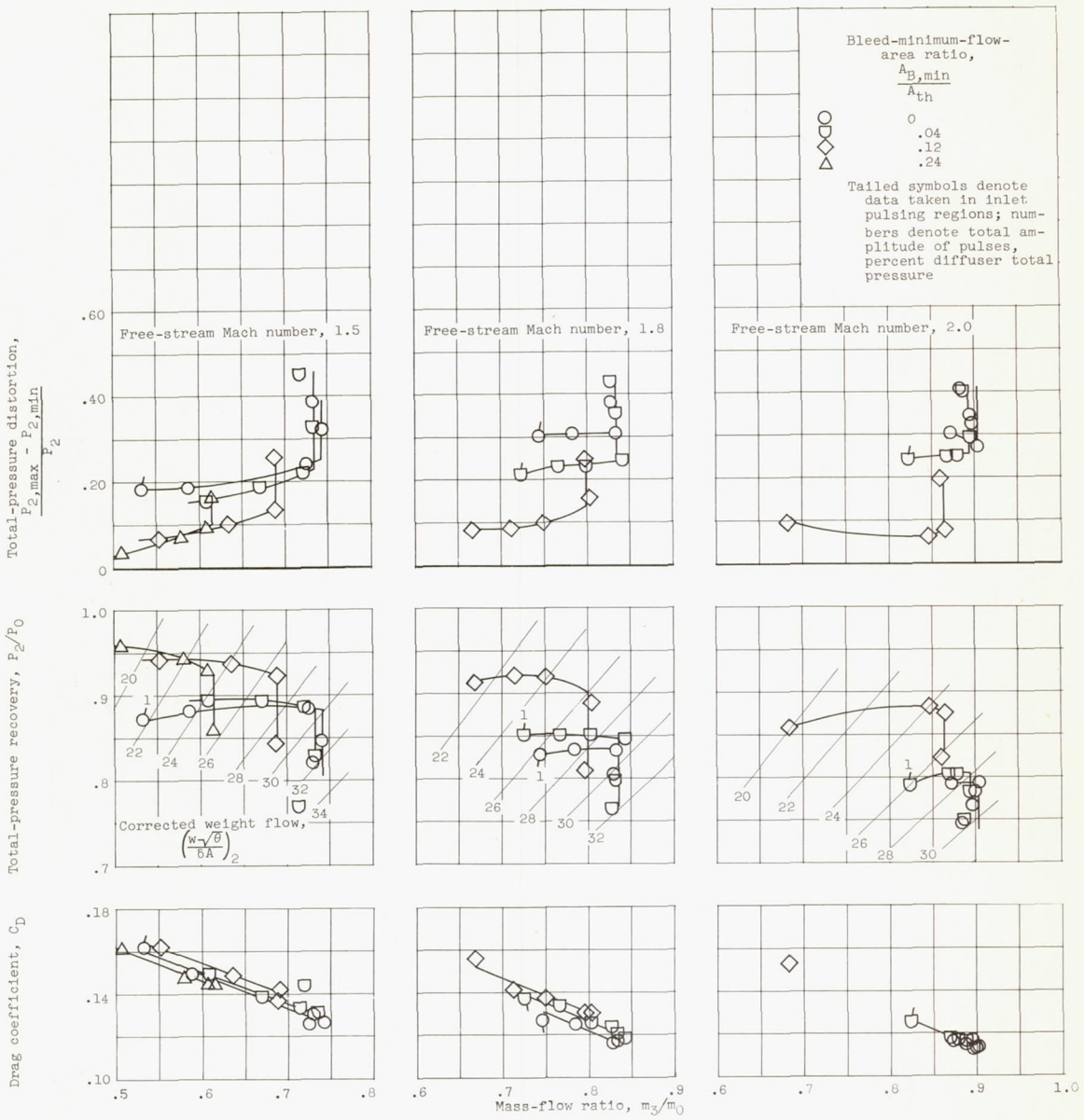

(b) External diverter height parameter, h/t, 1/3.

Figure 6. - Continued. Inlet performance characteristics of forward ram scoop having 14° ramp with side fairings (configuration A-2).

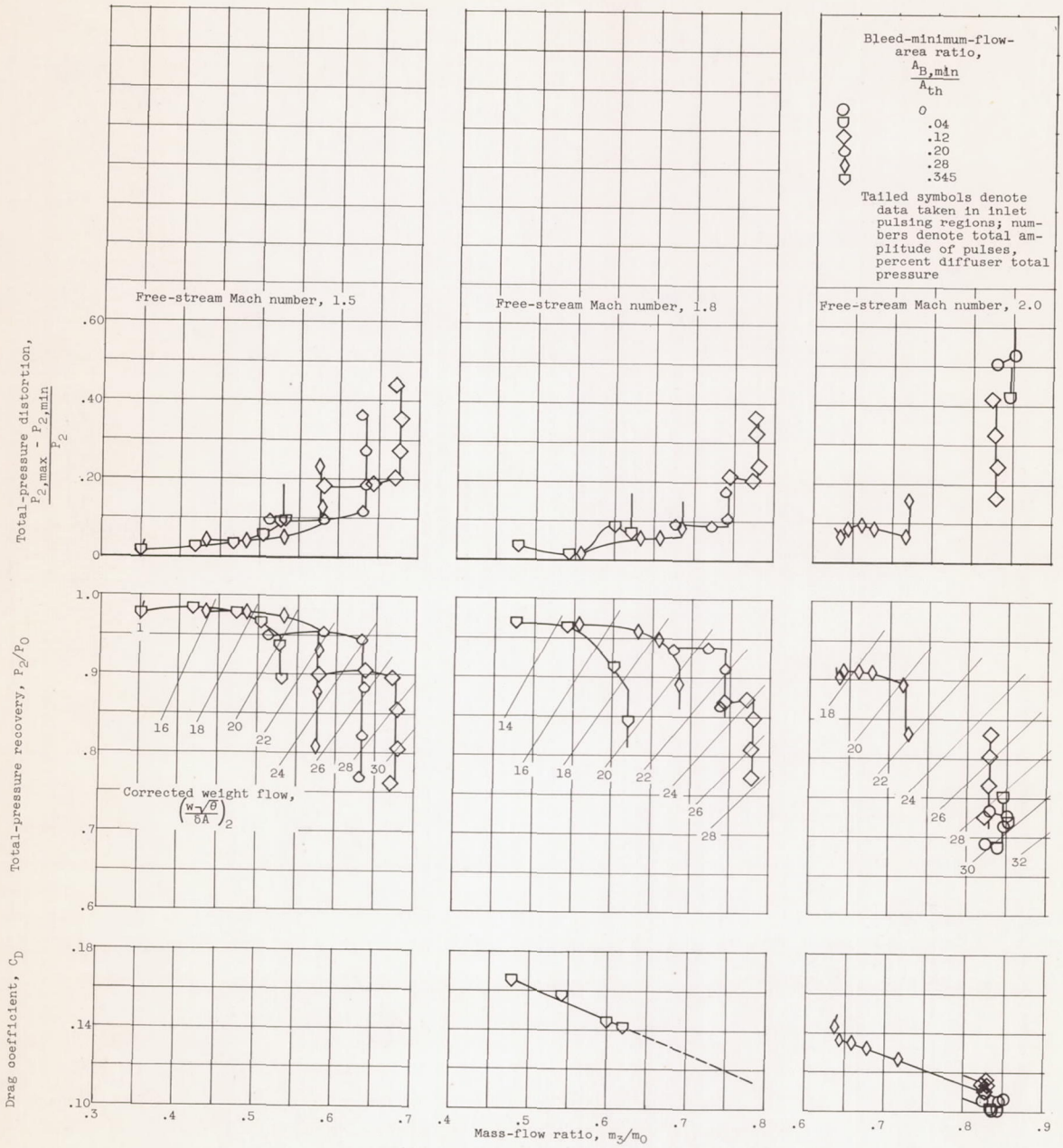

(c) External diverter height parameter, h/t, 0.

Figure 6. - Concluded. Inlet performance characteristics of forward ram scoop having 14° ramp with side fairings (configuration A-2).

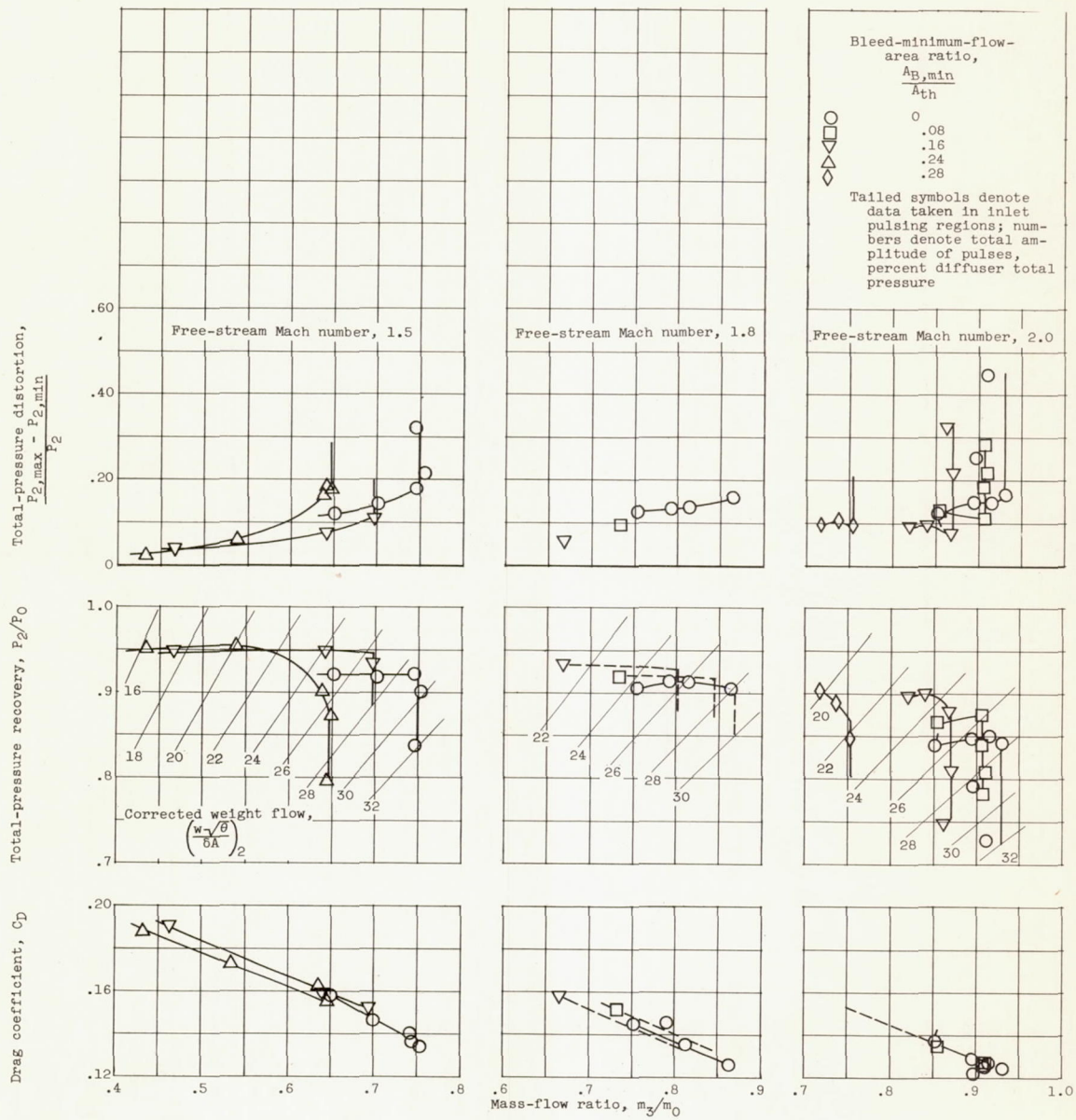

(a) External diverter height parameter, h/t, 1.

Figure 7. - Inlet performance characteristics of aft ram scoop having 14° ramp with side fairings (configuration B-2).

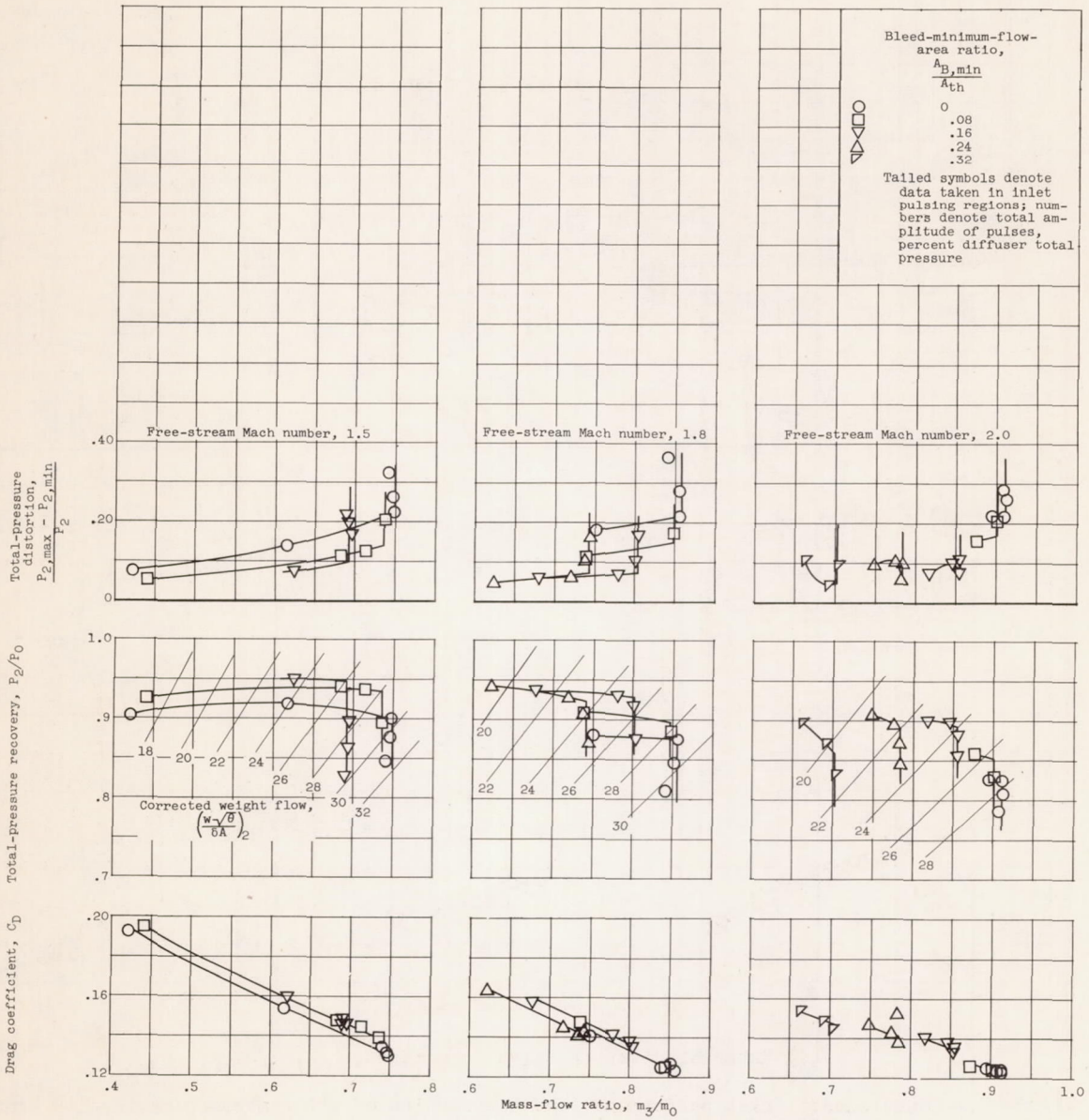

(b) External diverter height parameter, h/t, 2/3.

Figure 7. - Continued. Inlet performance characteristics of aft ram scoop having 14° ramp with side fairings (configuration B-2).

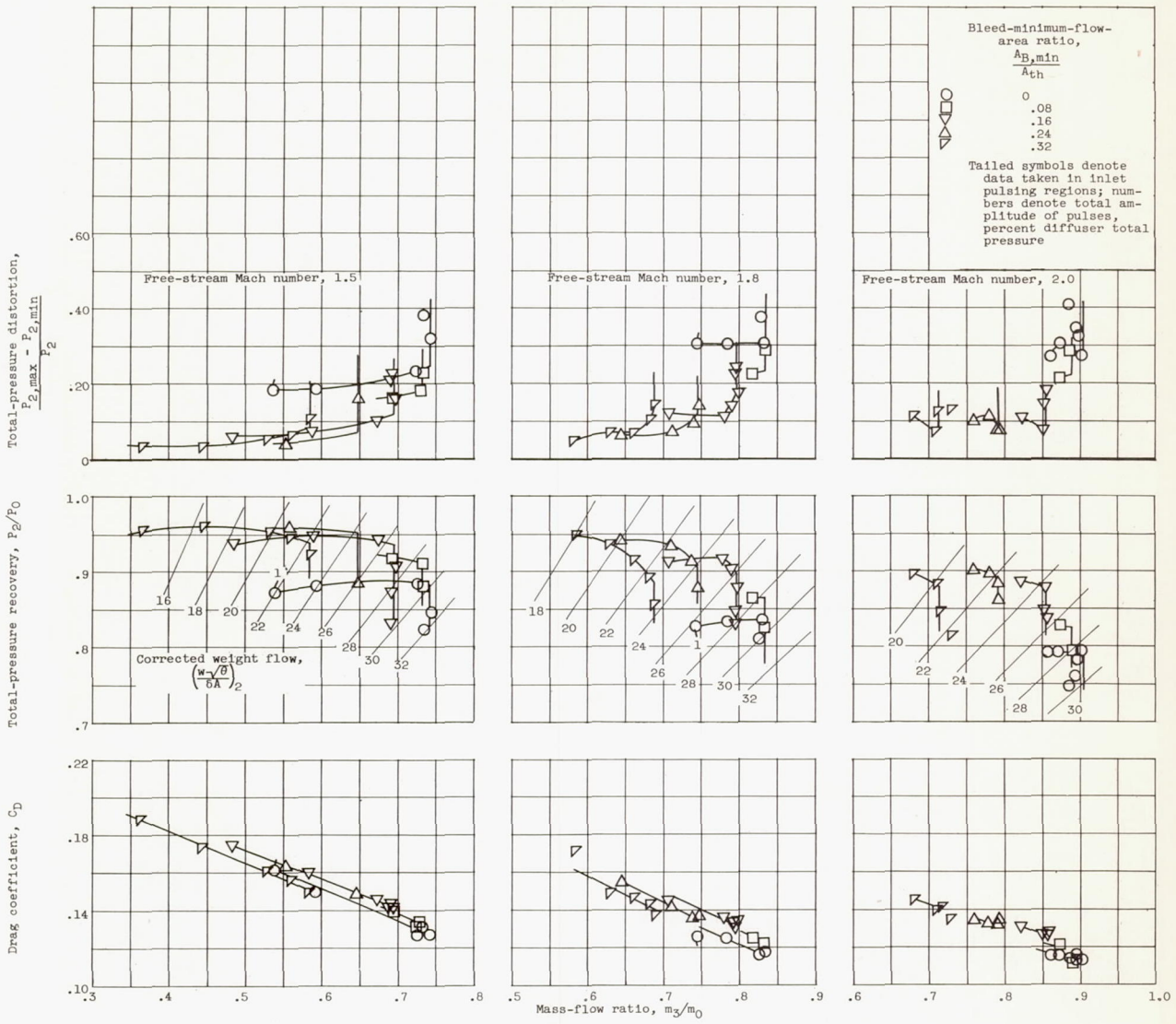

(c) External diverter height parameter, h/t, 1/3.

Figure 7. - Concluded. Inlet performance characteristics of aft ram scoop having 14° ramp with side fairings (configuration B-2).

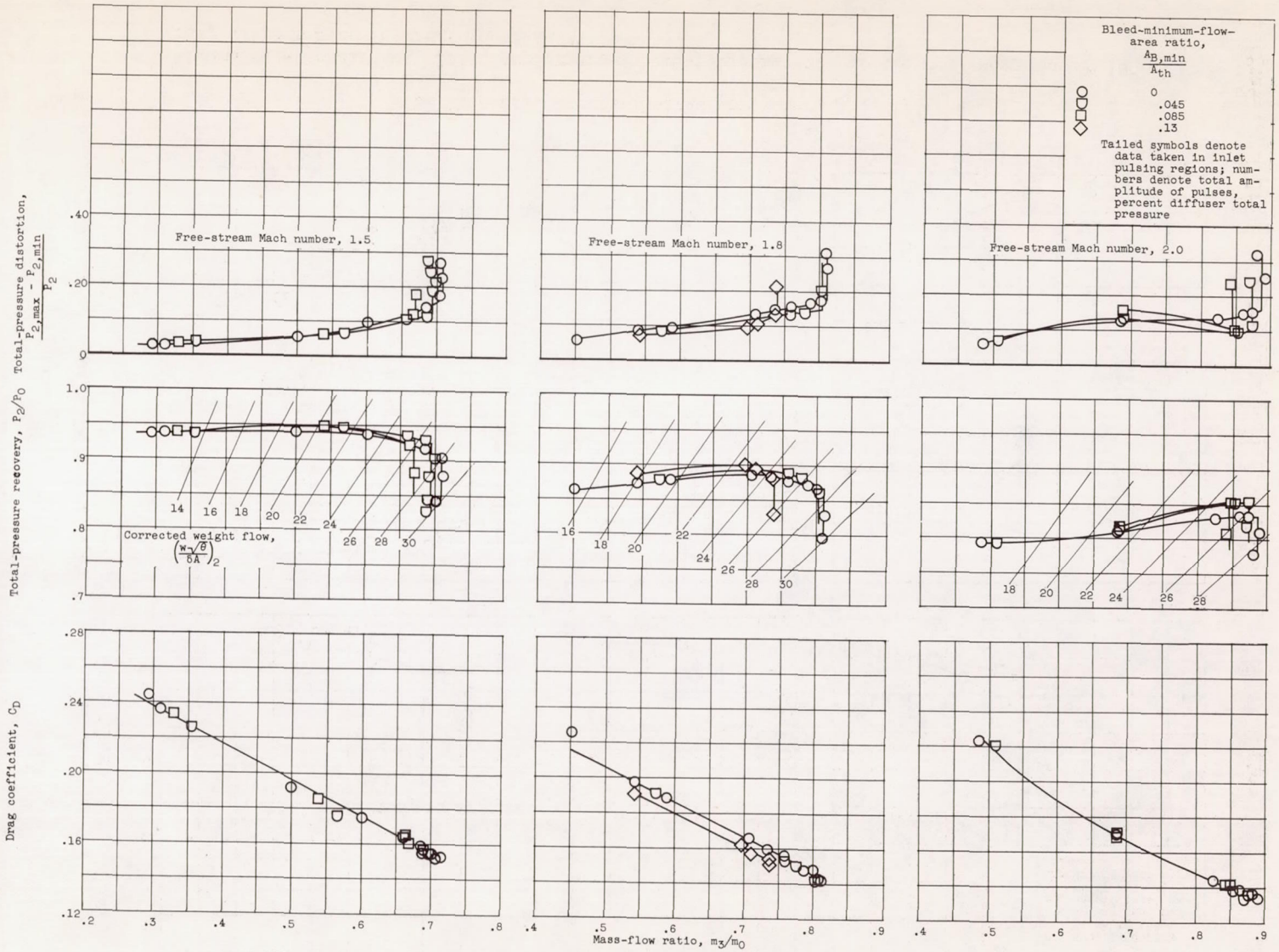

(a) External diverter height parameter, h/t, 1.

Figure 8. - Inlet performance characteristics of forward ram scoop having 18° ramp without side fairings (configuration C-1).

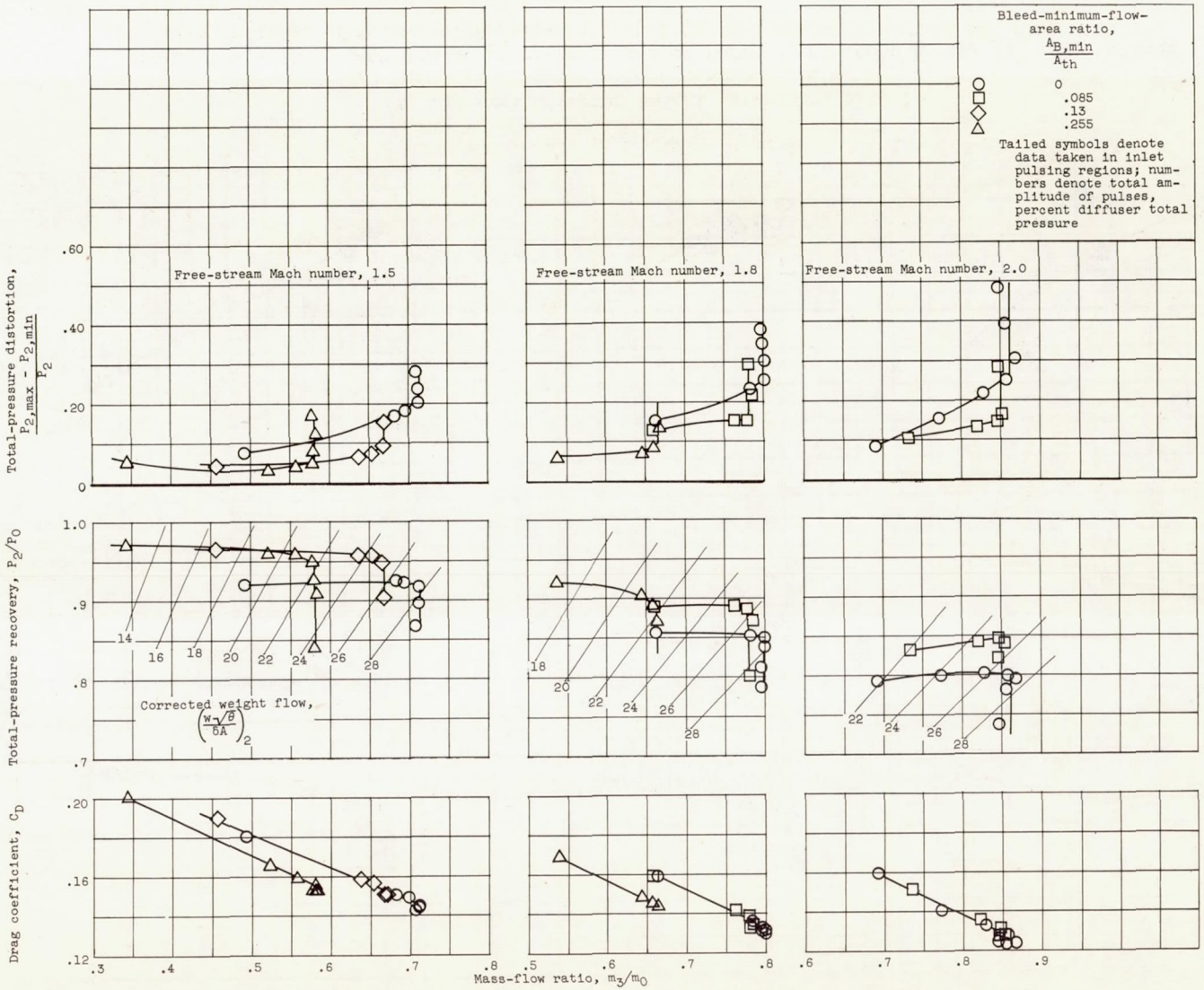

(b) External diverter height parameter, h/t, 1/3.

Figure 8. - Concluded. Inlet performance characteristics of forward ram scoop having 18° ramp without side fairings (configuration C-1).

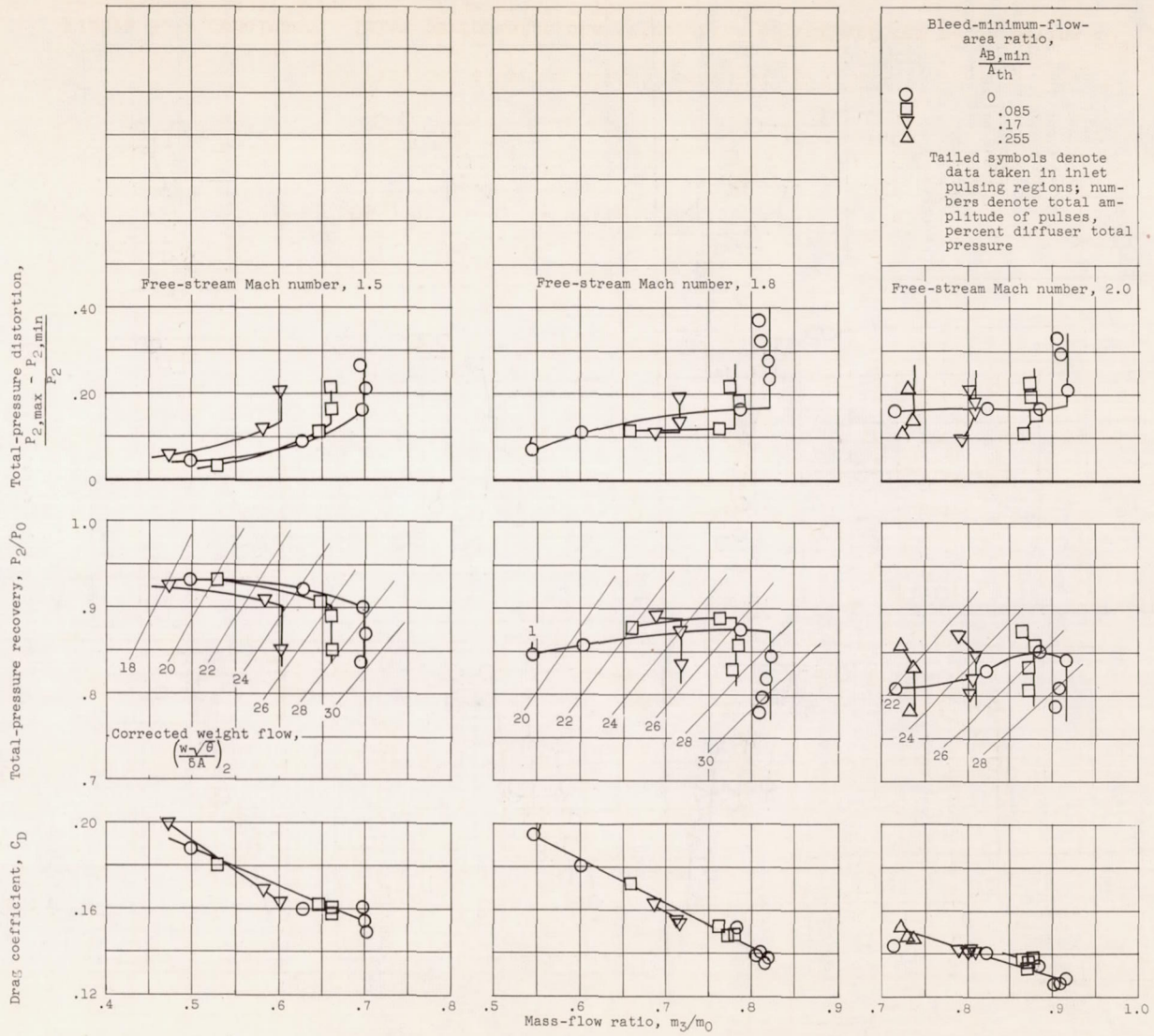

(a) External diverter height parameter, h/t, 1.

Figure 9. - Inlet performance characteristics of forward ram scoop having 18° ramp with side fairings (configuration C-2).

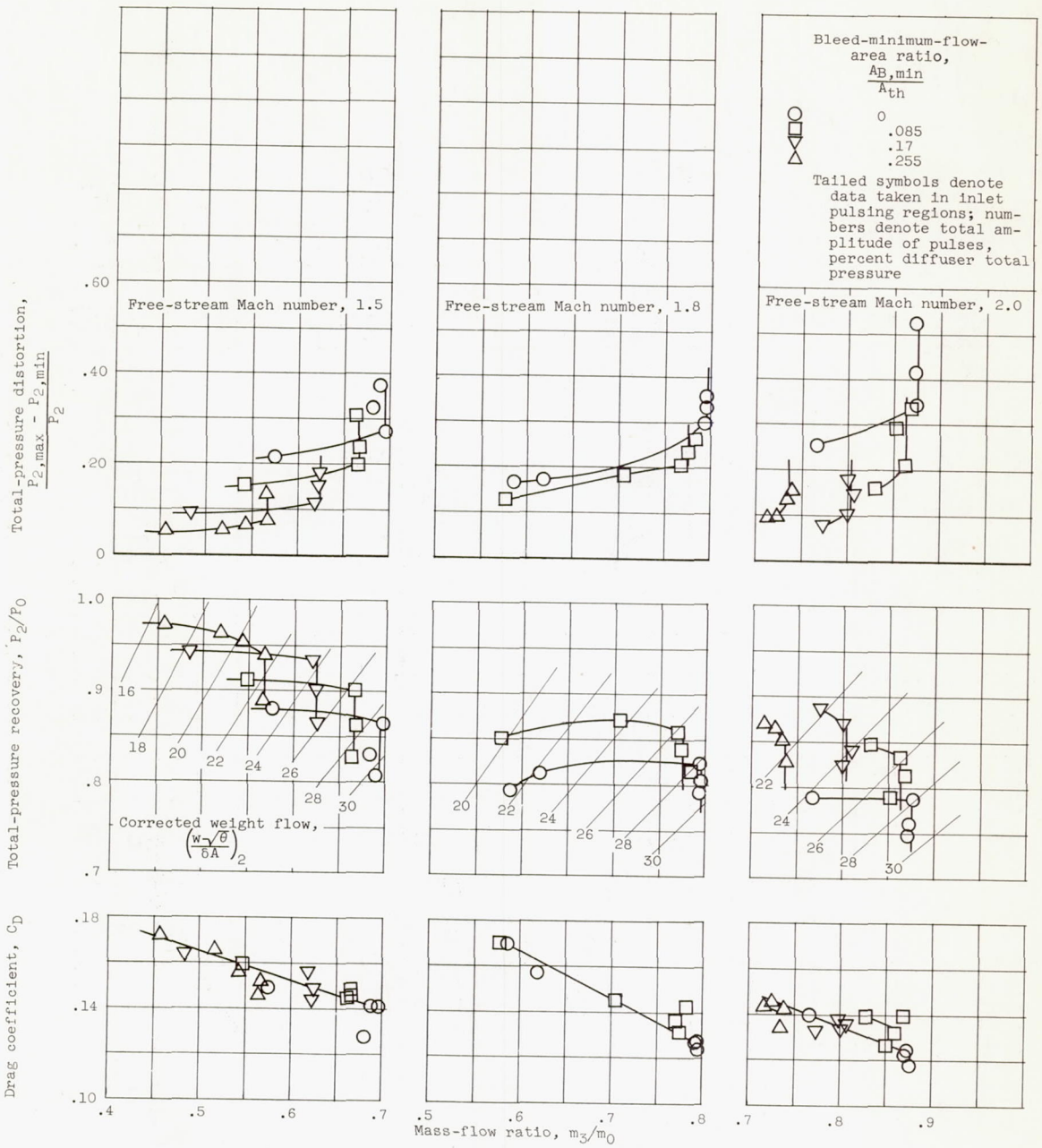

(b) External diverter height parameter, h/t, 1/3.

Figure 9. - Concluded. Inlet performance characteristics of forward ram scoop having 18° ramp with side fairings (configuration C-2).

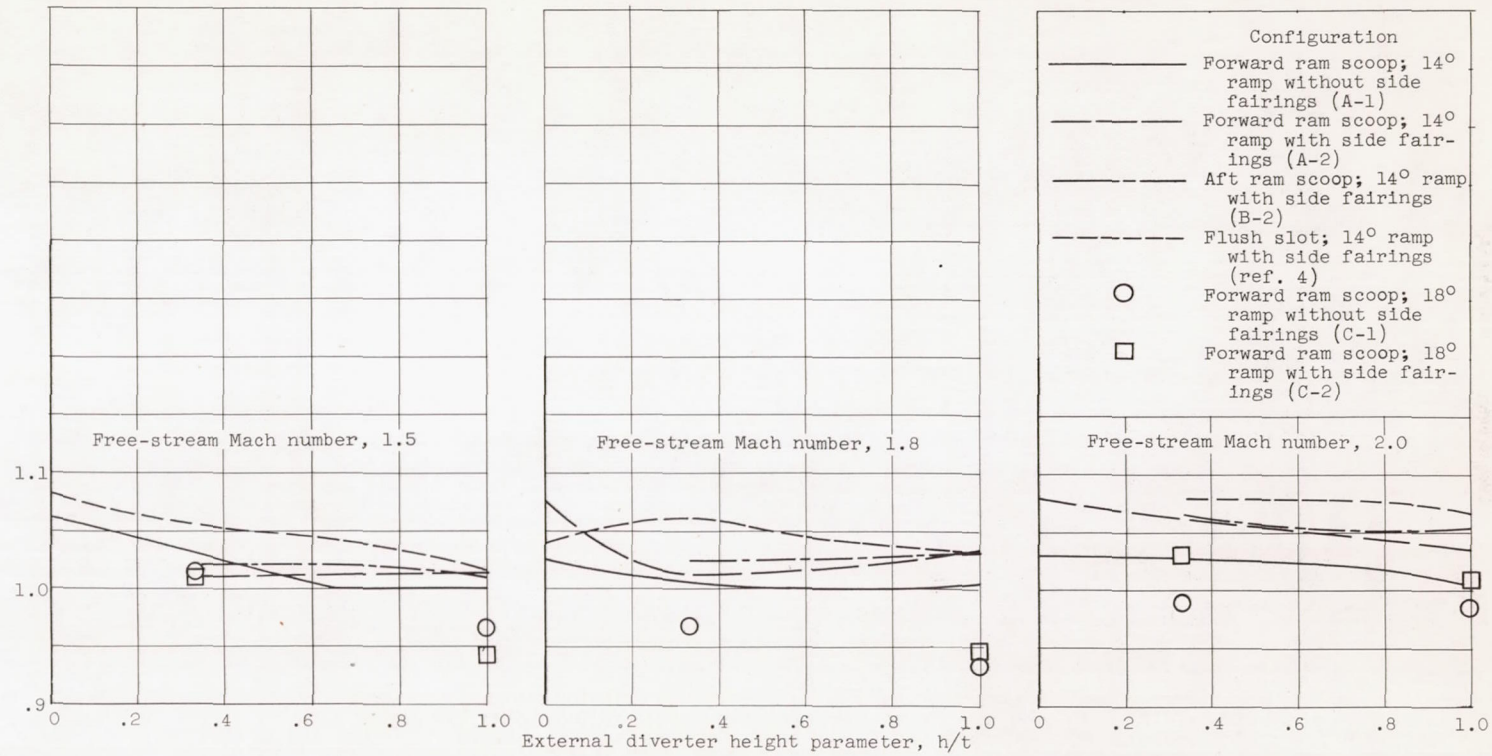

Figure 10. - Thrust parameter at optimum bleed for various configurations.